Am J Physiol Gastrointest Liver Physiol 302: G598–G607, 2012.
First published December 29, 2011; doi:10.1152/ajpgi.00330.2011.

Role of myosin Va in purinergic vesicular neurotransmission in the gut

Arun Chaudhury, Xue-Dao He, and Raj K. Goyal

Center for Swallowing & Motility Disorders, Veterans Affairs Boston HealthCare System and Harvard Medical School, Boston, Massachusetts

Submitted 22 August 2011; accepted in final form 23 December 2011

Chaudhury A, He XD, Goyal RK. Role of myosin Va in purinergic vesicular neurotransmission in the gut. *Am J Physiol Gastrointest Liver Physiol* 302: G598–G607, 2012. First published December 29, 2011; doi:10.1152/ajpgi.00330.2011.—We examined the hypothesis that myosin Va, by transporting purinergic vesicles to the varicosity membrane for exocytosis, plays a key role in purinergic vesicular neurotransmission. Studies were performed in wild-type (WT) and myosin Va-deficient *dilute, brown, nonagouti* (DBA) mice. Intracellular microelectrode recordings were made in mouse antral muscle strips. Purinergic inhibitory junction potential (pIJP) was recorded under nonadrenergic noncholinergic conditions after masking the nitrergic junction potentials. DBA mice showed reduced pIJP but normal hyperpolarizing response to P2Y1 receptor agonist MRS-2365. To investigate the mechanism of reduced purinergic transmission in DBA mice, studies were performed in isolated varicosities obtained from homogenates of whole gut tissues by ultracentrifugation and sucrose cushion purification. Purinergic varicosities were identified in tissue sections and in isolated varicosities by immunostaining for the vesicular ATP transporter, the solute carrier protein SLC17A9. The varicosities were similar in WT and DBA mice. Myosin Va was markedly reduced in DBA varicosities compared with the WT varicosities. Proximity ligation assay showed that myosin Va was closely associated with SLC17A9. Vesicular exoendocytosis was examined by FM1–43 staining of varicosities, which showed that exoendocytosis after KCl stimulation was impaired in DBA varicosities compared with WT varicosities. These studies show that SLC17A9 identifies ATP-containing purinergic varicosities. Myosin Va associates with SLC17A9-stained vesicles and possibly transports them to varicosity membrane for exocytosis. In myosin Va-deficient mice, purinergic inhibitory neurotransmission is impaired.

vesicular exocytosis; intracellular motors; neurotransmission; SLC17A9; myosins

NEUROTRANSMISSION IS ACCOMPLISHED by the release of neurotransmitters from bulbous nerve endings of neurons called varicosities. Vesicular neurotransmitters are stored in secretory vesicles and released by exocytosis at the varicosity membrane. In 1970, Burnstock (11) first proposed that ATP may serve as a vesicular cotransmitter with other well-established vesicular neurotransmitters. Purinergic neurotransmission involving a wide variety of purinoreceptors has now been observed throughout the central and peripheral nervous systems (9).

Although ATP itself is generally thought to be the purinergic transmitter candidate, the nucleotide that may produce purinergic response on target cells may be its breakdown product ADP (9). Recently, another nucleotide, β-nicotinamide adenine dinucleotide (NAD) has been proposed as a purinergic transmitter (31). However, the evidence for β-NAD rather than ATP/ADP being the purinergic transmitter is questionable (18).

Address for reprint requests and other correspondence: R. K. Goyal, Harvard Medical School, VA Medical Ctr., 1400 VFW Parkway, West Roxbury, MA 02132 (e-mail: raj_goyal@hms.harvard.edu).

At neuromuscular junctions, ATP is thought to be a cotransmitter with other neurotransmitters, including acetylcholine (ACh), tachykinin, and nitric oxide (NO) (8, 10, 35). ATP may produce either excitatory or inhibitory responses depending on the type of purinergic receptors present on the target cells (3, 9).

Until recently, identification of purinergic varicosities has been difficult because of lack of a suitable marker. Recently, however, immunostaining of SLC17A9 has provided an important tool in localizing neural and nonneural cells that transport ATP into vesicles (25). Recent studies have identified this vesicular nucleotide transporter (VNUT) as SLC17A9, a member of a large family of solute carrier (SLC) proteins (40).

The release of vesicular neurotransmitters requires translocation of the neurotransmitter-filled vesicles to the varicosity membrane for exocytosis (36). New immature peptidergic dense core vesicles are formed at the Golgi complex in somas of neurons and transported along the axon by kinesin motors on microtubule tracts to the varicosity (5). Within the varicosity, the vesicles are first filled with neurotransmitters and probably ATP and then carried by myosin motors along the F-actin tracts to the varicosity membrane. At the varicosity membrane, the vesicles undergo Ca^{2+}-dependent exocytosis and neurotransmitter release (5, 7, 22, 36).

Myosin motors form a large superfamily of motor proteins (4, 16). Myosins have distinctive molecular structure and cargo specificity (21, 48). Various unconventional myosins have been shown to play important roles in the process of exocytosis, including in neuronal cells (38). Different kinds of myosins, including myosins II, Va, Vb, and VI, have been shown to participate in vesicular exocytosis and endocytosis (16, 21, 32, 44). Myosin Va has been shown to be widely expressed in many presynaptic and postsynaptic neurons in the central and the peripheral nervous systems and constitute almost 0.3% of all proteins in the brain (13). In the rat, myosin Va is localized in motor nerve fibers emanating from myenteric plexus (14, 27). However, the role of myosin Va in enteric varicosities remains unknown.

Myosin Va is well known to transport melanosome, organelles such as endoplasmic reticulum and trans-membrane proteins to dendritic spine in the postsynaptic neuron (26, 50). The phenotype of myosin deficiency includes defective skin pigmentation and a variety of neurological disorders, including ataxic gait and clonic seizures (30). Syndromes of myosin deficiency are seen in many animal species, including humans (Griscelli syndrome type 1) (49) and horses (lavender foal syndrome) (6).

In the mouse, deletion of the MYO Va gene results in the so called "dilute lethal" mutant mice that die soon after birth (28). Partial deficiency of myosin Va results in the so-called surviving hypomorphic mutant *dilute, brown, nonagouti* (DBA) mice (23, 42). We have recently reported that DBA mice have

impaired enteric nitrergic neurotransmission due to defective transport of the enzyme neuronal nitric oxide synthase (nNOS)-α to the varicosity membrane (12). Our preliminary studies suggested that purinergic inhibitory junction potential (pIJP) may also be reduced in DBA mice. The purpose of the present study was to identify purinergic nerve terminals and to examine the role of myosin Va in vesicular transport and purinergic inhibitory neurotransmission.

MATERIALS AND METHODS

All experiments were preapproved by the Institutional Animal Care and Use Committee at Veterans Affairs Boston HealthCare System.

Animals

Four- to six-week-old male wild-type (WT) C57BL/6J mice (genotype B/B, D/D) with normal black hair color served as controls. Male DBA/2J (genotype b/b, d/d) were used as models of myosin Va deficiency.

Chemicals

All chemicals were obtained from Sigma Chemical (St. Louis MO). {(1*R*,2*R*,3*S*,4*R*,5*S*)-4-[6-amino-2-(methylthio)-9*H*-purin-9-yl]-2,3-dihydroxybicyclo[3.1.0]hex-1-yl}methyl diphosphoric acid mono ester trisodium salt (MRS-2365) and (1*R**,2*S**)-4-[2-chloro-6-(methylamino)-9*H*-purin-9-yl]-2-(phosphonooxy)bicyclo[3.1.0]hexane-1-methanol dihydrogen phosphate ester diammonium salt (MRS-2279) were obtained from Tocris Biosciences (Ellisville, MO).

Intracellular Recordings

Intracellular membrane potentials of gastric antrum were recorded using glass microelectrodes (1.2 mm OD; FHC, Brunswick, ME) with tip resistance between 30 and 80 MΩ. The microelectrode was connected to a high-impedance electrometer (DUO 773; WPI). Inhibitory junction potentials (IJPs) were recorded under nonadrenergic noncholinergic (NANC) conditions, adding atropine (1 μM) and guanethidine (5 μM) to the bath solution. N^G-nitro-L-arginine (L-NNA, 100 μM)-containing solution was perfused to mask the nitrergic slow IJP. Transmural stimulation was performed using the following stimulus parameters: 70-volt, 1-ms-duration square pulses at 20 Hz for 0.5 s. Agonists/antagonists were injected into the bath to achieve final concentrations as indicated.

Preparation of Enteric Varicosities

Varicosities were obtained from the subdiaphragmatic portion of gut of WT and DBA mice and used for experiments as described previously (12). Gut tissues from 30 WT mice and 18 DBA mice were used to prepare six independent homogenates of varicosity materials.

Antibodies

The following primary antibodies were used: myosin Va [S-14 that detects a 12–20 peptide region in the region encoded by exon E in the tail region spanning AA 1350–1400 (lot no. B2108, goat; Santa Cruz Biotechnology)], VNUT solute carrier isoform 17A9 (SLC17A9, lot no. 001, rabbit; MBL International), nNOS (COOH-terminal specific polyclonal antibody, lot no. 952416, goat; Abcam), nNOSα (NH_2-terminal specific K-20, lot no. J1606, rabbit; Santa Cruz Biotechnology), vesicular acetylcholine transporter (vAChT, lot no. H1209, goat; Santa Cruz Biotechnology), and synaptophysin (lot no. 313996, rabbit; Abcam). Appropriate species-specific secondary antibodies were used [donkey anti-goat AlexaFluor594 (lot no. 714270) and goat anti-rabbit AlexaFluor 488 (lot no. 828814) (Molecular Probes)]. Secondary antibodies were chosen bound to fluorophores with nonoverlapping emission spectra. Anti-rabbit photostable quantum dot-tagged (Qdot 605, lot no. 813625; Molecular Probes) secondary antibody was used for myosin Va imaging to facilitate quantitative comparisons. For actin staining, phalloidin AlexaFluor 488 (lot no. 808465; Molecular Probes) was used. The vial contents containing the lyophilized solid were dissolved in 0.75 ml methanol. Five microliters of this stock solution of the fluorescent phallotoxin were diluted into 200 μl PBS-BSA for staining. The antibody used for identifying SLC17A9 (MBL International) was specific for SLC17A9. It was raised against a peptide derived from near the COOH-terminal region of human SLC17A9 isoform2, which is identical to the mouse SLC17A9 peptide and is characterized by the peptide sequence GIVL (47). The primary antibody was raised in a rabbit species and affinity purified. SLC17A9 belongs to the major facilitator family of proteins SLC17 but has minimal overlap with peptide sequences of other members of this family that carry different peptide sequences like R-DE. Omitting this primary antibody did not show a signal in the enteric varicosities. A blocking peptide was also used to test the specificity of staining with this SLC17A9 antibody. Specificity of the other antibodies used in this study has been tested earlier in the laboratory by running Western blots of positive controls or colocalization with antibodies raised against a different region of the peptide.

Staining of Whole Mounts of Antral Muscle Strips with SLC17A9 Antibody

Stomach was removed, and 6 mm × 6 mm wide strips of smooth muscle layer were prepared under the stereomicroscope by shearing the mucosa. These muscle strips underwent immersion fixation in the cold with 4% paraformaldehyde. The strips were thereafter washed in PBS buffer containing 0.01% Tween 20 and blocked in a PBS buffer containing bovine serum albumin. Furthermore, these strips were incubated with 1 in 200 SLC17A9 primary antibody diluted in PBS-BSA buffer at 4°C for 2 days, followed by incubation with appropriate species-specific Alexa-Fluor488-conjugated secondary antibody (1 in 2,000) for 1 day at 4°C. Pilot experiments were run to determine the concentrations of the primary and secondary antibodies. In separate experiments, muscle strips were incubated with primary antibodies that were mixed with a blocking peptide (mol wt 2009.33, 90% purity as measured by HPLC) for 2 h before floatation of the tissue strips. Washes were done between changing primary and secondary antibodies. Tissue strips were mounted on clear glass slides with UltraCruz mounting medium and imaged under confocal mode (Zeiss Axiovert S100 inverted microscope) using ×20 apochromat [numerical aperture (NA) 0.8] dry objectives.

Staining Protocol of Varicosities for Immunohistochemistry

The protocol was adapted from Panfoli et al. (33), standardized in the laboratory, and recently reported (12).

Visualization of Varicosities with Confocal Laser Microscope

Confocal imaging was performed to obtain spatial information of distribution of fluorophores in the varicosities by eliminating out-of-focus fluorescence. The samples on glass were imaged with an inverted Nikon microscope (ECLIPSE TE2000-U; Nikon) interfaced with a confocal system (Nikon C1) and Melles-Griot lasers carrying 488- and 595-nm lines (bandwidth 515/30 and 590/50). Varicosities were visualized with a X20–63 water immersion or a ×100 oil objective fitted with differential interference contrast optics (NA 0.7–1.4). The diopter adjustment ring was turned so that the double crosshairs and the varicosities came into focus. Structures were localized under brightfield illumination to minimize loss of fluorescence and subsequently imaged under confocal modes with a minimum pinhole diameter (this step was rigorously followed during live varicosity imaging after FM staining). The microscope is located on a vibration isolation chamber

(Micro40/60 series; Halcyonics), and the door was locked during imaging to shut out ambient light. High-quality images were obtained by averaging multiple frames, and imaging was stopped if quality diminished (<30 dB). Images were acquired through in-built photomultiplier tubes and visualized with a EZ-C1 viewer. For comparison of protein expression by quantitative comparison of fluorescence intensities, all acquisition parameters were the same between WT and DBA groups (starting from the concentration of primary antibodies). Images with only a high signal-to-noise ratio and minimal background were used for analyses. Image analyses and colocalization parameters as well as linear measurements on unscaled tiff files of raw images were performed with ImageJ (United States National Institutes of Health, Bethesda, MD). For presentation of low-magnification images of varicosities, slight changes of fluorescence saturation were made in certain representative panels, and outlined in the legends for Figs. 1–7. As outlined above, integrated densities of red-green fluorescence were estimated on raw tiff images with ImageJ.

In Situ Proximity Ligation Assay

For examining protein-protein interactions, proximity ligation assay (PLA) was performed, and PLA blobs were quantitated as recently described (12). Freshly plated WT and DBA varicosities were studied using the Duolink in situ PLA detection kit (Olink, Uppsala, Sweden). Varicosities were examined to detect interactions of myosin Va with SLC17A9.

FM1–43 Labeling of Varicosities for Exoendocytosis Activity

Exoendocytosis in plated live enteric varicosities was performed by labeling varicosities with the styryl dye FM1–43 at room temperature using previously described protocols (17). Varicosities were exposed to 5 μM FM1–43 diluted in Krebs' buffer containing 50 μM KCl in the dark for 5 min at room temperature. After that, nerve terminals were treated with Ca^{2+}-free buffer containing the dye for 15 min. This was followed by three washes with fresh saline solution for 5 min each. Imaging was performed taking care not to expose plates (now bathed in Krebs' buffer) to light. To prevent photobleaching of the signals, intermittent time-lapse imaging of varicosities was performed, and confocal imaging was performed using minimal laser power in the minimal pinhole mode. The degree of labeling indicated exoendocytosis. This preparation was then exposed to high K^+ (50–100 mM) for 10 min, in the absence of extracellular FM1–43 dye, to exocytose labeled vesicles. High K^+ treatment completely destained the varicosities, indicating that FM1–43 staining was due to the labeled vesicles.

Statistics

Unpaired Student's *t*-test for asymmetric *n* values was used to compare significance of difference between means of myosin Va deficiency with WT samples. $P < 0.05$ was accepted as statistically significant. Correlation coefficients like Pearson and Manders' were used to estimate overlapping fluorescent signals during dual immunohistochemistry.

RESULTS

Purinergic Neuromuscular Neurotransmission in WT and DBA Mice

Resting membrane potential. The resting membrane potential (RMP) of the gastric smooth muscles in WT mice was -50 ± 1.2 mV ($n = 25$ recordings/5 mice), which was slightly different from -46 ± 0.5 mV in DBA ($n = 11$ recordings/5 mice) (2-tailed $P = 0.038$, unpaired *t*-test). This slight, but significant, reduction in resting membrane potential may result from defective nitric oxide synthesis in DBA mice, as recently reported (12).

Effect of β-NAD on RMP. To examine the potential role of β-NAD rather than ATP as a purinergic transmitter in the mouse stomach, we examined the effectiveness of β-NAD in causing membrane hyperpolarization. β-NAD was ineffective in producing hyperpolarization of gastric smooth muscles. The membrane potential after 50 mM β-NAD was -48.9 ± 2 vs. -48.3 ± 2 mV in control ($P = 0.05$; $n = 7$ recordings obtained from 3 mice). In contrast, *α,β-methylene-ATP* was highly effective in producing membrane hyperpolarization of the smooth muscles. The membrane potential was -50 ± 3.3 in the control and -59 ± 3.1 after 50 μM *α,β-methylene-ATP* ($P < 0.01$). These observations suggest that ATP or its product rather than β-NAD may be the inhibitory purinergic transmitter in the mouse stomach (18).

Purinergic (fast) IJP. Electrical field stimulation under NANC conditions elicited a compound IJP, which consisted of fast and slow components that were due to purinergic and nitrergic mediators, respectively. The fast pIJP was elicited in the presence of the nitrergic inhibitor L-NNA. The purinergic fast IJP was -17.6 ± 0.5 mV in the control mice (25 recordings in 5 mice) and -7.1 ± 1.2 mV in the DBA mice (11 recordings in 5 mice). This decrease in the DBA was highly significant ($P < 0.0001$) (Fig. 1). PIJP was suppressed by the P2Y1 receptor antagonist MRS-2279 (5 μM) (-17.1 ± 0.5 vs. -0.5 ± 0.1, before and after MRS-2279, mean of 11 recordings in 4 mice).

Hyperpolarization to purinergic agonists. To determine whether the reduced pIJP was due to a postjunctional defect in the smooth muscles of DBA mice or due to reduced release of the purinergic transmitter, we examined the smooth muscle hyperpolarizing responses to purinergic agents ATP and the selective PY1 receptor agonist MRS-2365. ATP (33 μM) induced hyperpolarization of -10 ± 0.6 mV in the WT mice (6 recordings/3 mice) and -9.2 ± 0.8 mV in the DBA mutants (6 recordings/3 mice) ($P > 0.05$). In WT mice, MRS-2365 (33 μM) induced hyperpolarization of -10.5 ± 1.0 mV (6 recordings/3 mice) and -10.7 ± 1.0 mV in the DBA mutants (3 recordings/3 mice) ($P > 0.05$) (Fig. 1). The effects of P2Y1 receptor stimulation were suppressed by the P2Y1 antagonist MRS-2279.

SLC17A9 Staining of Varicosities in Whole Mount

Examination of whole mounts of antral smooth muscle strips showed that SLC17A9 staining was seen in varicosities along nerve fibers distributed in the muscle wall, the varicosities similar in appearance to that described for nitrergic varicosities (45) (Fig. 2). Note that smooth muscle fibers remained unstained. Preincubation of the primary antibody with blocking antibody resulted in lack of staining of varicosities (data not shown).

Enteric Varicosities in WT and DBA Mice

To investigate the mechanism of impaired purinergic inhibitory neurotransmission, studies were performed in isolated varicosities in WT and DBA mice. In WT mice, under bright-field illumination, varicosities appeared rounded or oval in shape with a mean diameter of 3.45 μm ($n = 500$ from 3 different pools). Identity of the varicosities was confirmed by

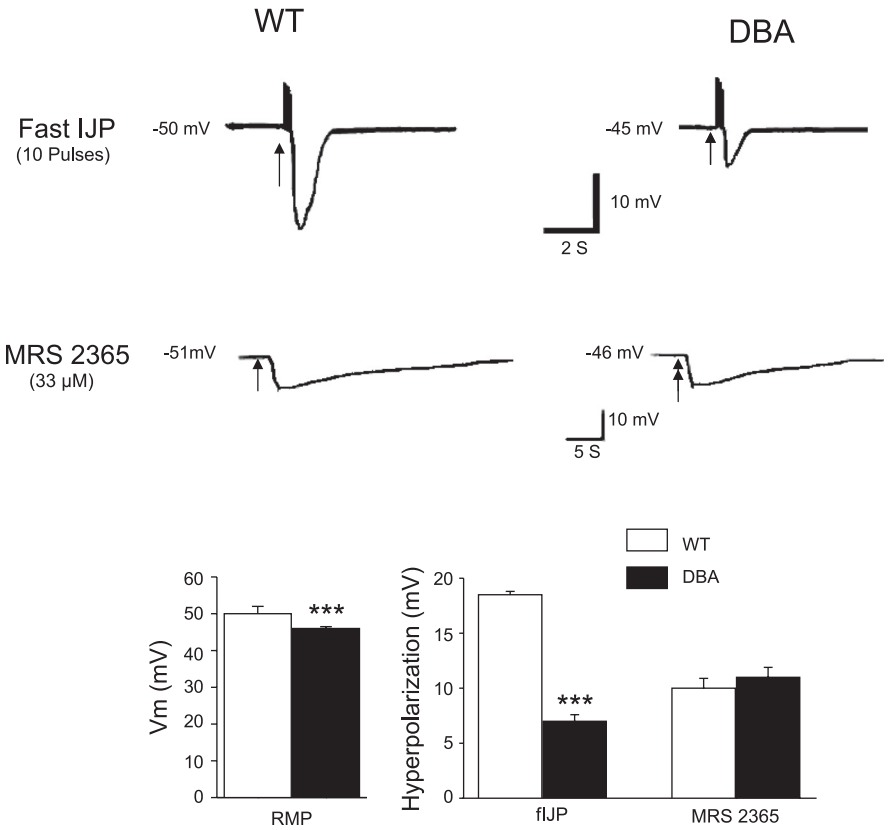

Fig. 1. Purinergic [fast (f)] inhibitory junction potential (IJP) and smooth muscle hyperpolarization to P2Y1 agonist, MRS-2365, in the antral smooth muscle in wild-type (WT) and *dilute, brown, nonagouti* (DBA) mice. *Top*: examples of the purinergic fIJPs. *Middle*: examples of hyperpolarizing responses to P2Y1 agonist MRS-2365. *Bottom*: cumulative data on the resting membrane potentials (V_m), amplitudes of fIJP, and hyperpolarization due to MRS-2365. Bars represent mean values ± SE. Note that, compared with WT mice, the purinergic IJP was markedly reduced in the DBA mice. On the other hand, hyperpolarization to P2Y1 agonist MRS-2365 was not affected in DBA mice. These observations show that, in myosin Va-deficient DBA mutant mice, purinergic neuromuscular neurotransmission is impaired due to possible impaired ATP release by the prejunctional enteric varicosities.

staining with synaptophysin. Varicosities from DBA mice were not different from the WT mice (Fig. 3). The mean diameter of varicosities in DBA mice was 3.39 μm (n = 500, from 3 different pools). This value is similar to that of the WT varicosities ($P > 0.05$). A distribution plot of the different sizes of the varicosities obtained from WT and DBA mice is also shown in Fig. 3.

Purinergic Nature of the Isolated Varicosities

We immunostained the enteric varicosities for VNUT SLC17A9 to establish the purinergic nature of the varicosities. SLC17A9 was localized to enteric varicosities (Fig. 4). This is the first demonstration of distribution of the VNUT SLC17A9 in the nerve terminals of the gut muscularis externa.

Colocalization of ATP transporter with other neurotransmitters. To determine whether the VNUT SLC17A9 was localized to the inhibitory nitrergic varicosities, double staining was done for SLC17A9 and nNOS. In WT mice, varicosities that stained for nNOS also stained for SLC17A9 (Pearson's correlation coefficient 0.89, 94.5% overlap, respectively) (Fig. 4). We also examined whether SLC17A9 colocalized with vAChT in the excitatory varicosities. Double staining for SLC17A9 and vAChT showed the varicosities that stained for vAChT also stained for the SLC17A9 (Pearson's correlation coefficient 0.94, 96% overlap) (Fig. 4). These observations suggest that SLC17A9 was colocalized in both nitrergic and cholinergic varicosities. It was noted that, although several nitrergic or cholinergic varicosities colocalized with SLC17A9, many varicosities that were neither nitrergic nor cholinergic stained for SLC17A9, suggesting that ATP transporter may be present in a diverse pool of varicosities that do not contain nNOS or vAChT. Similar observations were made in DBA mice (data not shown).

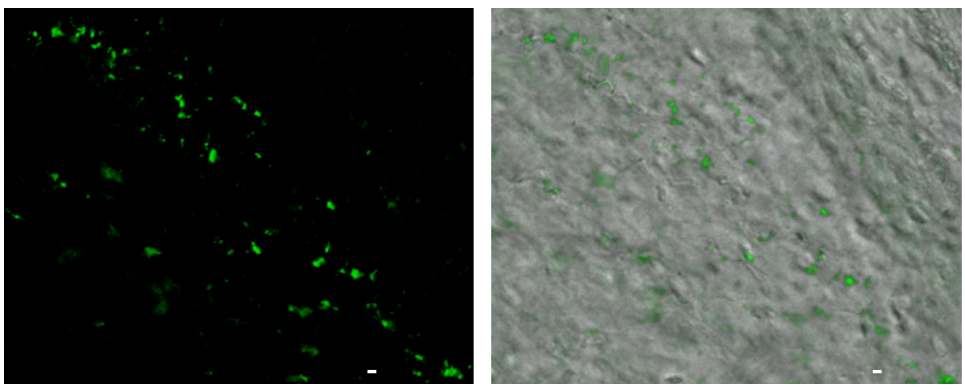

Fig. 2. SLC17A9 staining of nerve varicosities in whole mounts of gastric antral muscle strips. *Left*, cumulative image of a stack of 21 slices imaged by Z scanning under confocal mode. *Right*, merged image of confocal imaging of the varicosities with the transmitted light. Note the direction of the muscle fibers as they run from the lower left hand side diagonally upward. Scale bar, 3 μm.

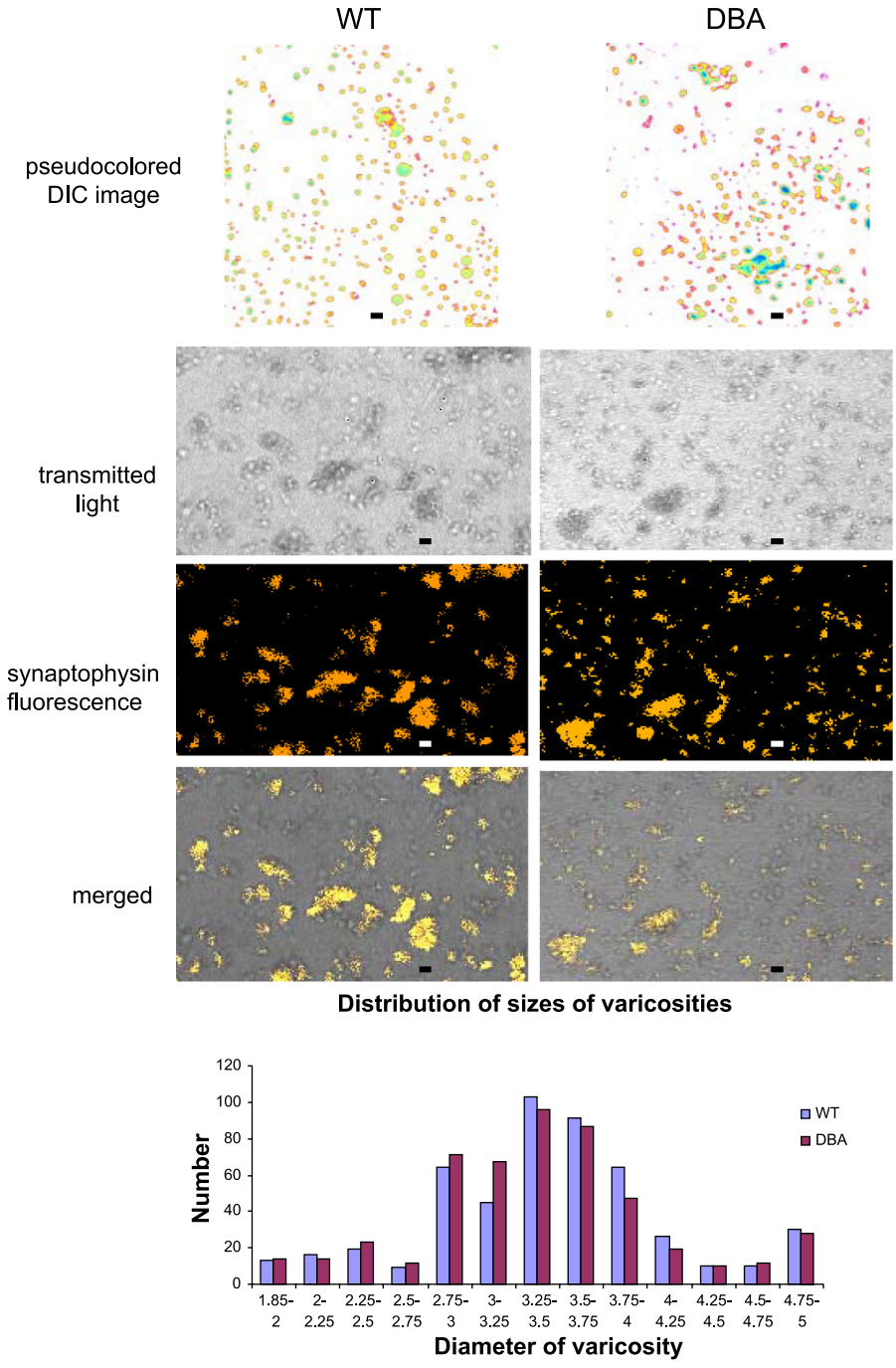

Fig. 3. Images of varicosities in WT and DBA mice. *Top*: pseudocolored differential interference contrast (DIC) images of plated varicosities viewed under low magnification. Note that varicosities appear similar in WT and DBA mice. *Middle*: transmitted light, synaptophysin fluorescence and merged image of a group of varicosities in WT and DBA mice. Note that both WT and DBA enteric varicosities stain for synaptophysin. Slight adjustment in saturation of fluorescence was performed for these representative images. Binned and plotted size distribution of varicosities in WT and DBA is shown in *bottom*. Note that there was no shift or change in varicosities of different sizes in the two groups. Scale bars, 3 μm.

Myosin Va in WT and DBA Enteric Varicosities

In WT enteric varicosities, myosin Va is widely distributed in a particulate fashion in both the cytosolic and perimembranous regions. In DBA mice, expression of myosin Va was significantly reduced or absent and required scanning of several fields for signal detection in terminals (Fig. 5). AlexaFluor488 conjugated to phalloidin was used to localize actin in the nerve varicosities. It was seen that myosin Va colocalized with actin in the WT varicosities (overlap >95%, Mander's A and B coefficients >0.9, n = 30). The secondary antibody used for myosin detection was quantum dot labeled, which allowed quantitative imaging of myosin Va signals. For quantitative imaging, unscaled tiff files were used without any change to settings of original acquisition parameters. Quantitative comparison of fluorescence intensities after background correction was performed as a surrogate marker for myosin Va protein expression. The fluorescence expression values in arbitrary units were normalized to surface areas of the varicosities. Compared with WT, DBA enteric varicosities nearly lacked expression of myosin Va (43.11 ± 4.5 in WT and 1.96 ± 0.67 in DBA, 2-tailed $P < 0.0001$, unpaired t-test, n = 400 WT and 515 DBA varicosities from 6 independent pools of varicosity samples).

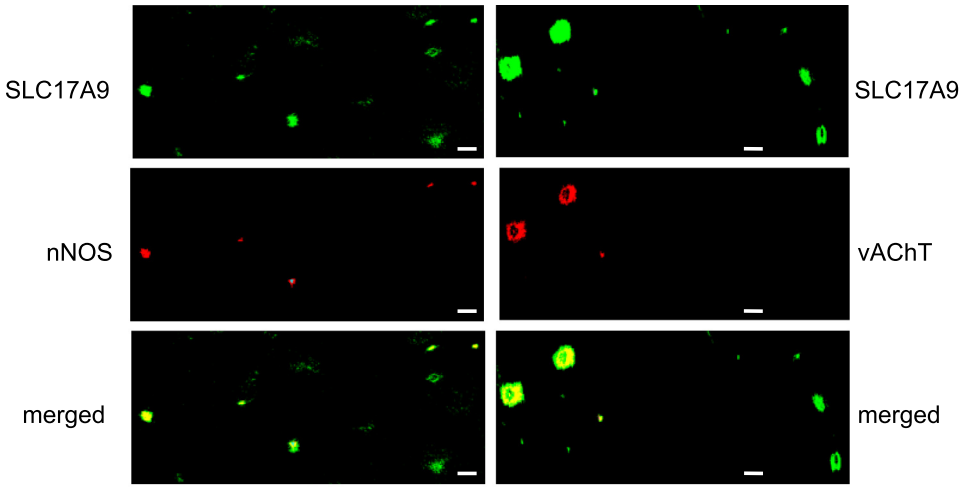

Fig. 4. Colocalization of vesicular nucleotide transporter SLC17A9 with the inhibitory neurotransmitter neuronal nitric oxide synthase (nNOS, *left*) and with the excitatory neurotransmitter marker vesicular acetylcholine transporter (vAChT, *right*) in WT enteric varicosities. *Top*: immunostaining with SLC17A9. *Middle*: staining for nNOS or vAChT. *Bottom*: merged images. Note that SLC17A9 was colocalized with both nNOSα- and VAChT-containing varicosities. Slight adjustment in saturation of fluorescence was performed for these representative images. Scale bars, 3 μm.

Association of Myosin Va with Purinergic Vesicle

Localization of myosin Va to SLC17A9 reactive varicosities. To specifically examine the colocalization of myosin Va in the purinergic terminals, WT varicosities labeled with myosin Va were probed for colocalization with SLC17A9. Figure 6*A* shows a high degree of colocalization of myosin Va with SLC17A9 (Pearson's correlation coefficient 0.9, 98.7% overlap). In contrast, because of the paucity of myosin Va in DBA mice, SLC17A9 was present without myosin Va (Fig. 6*A*).

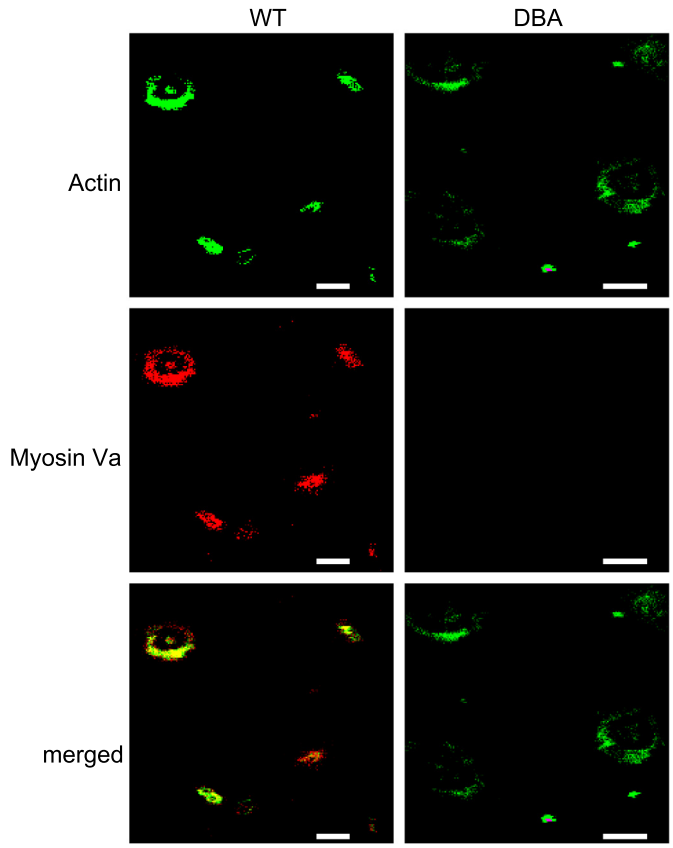

Fig. 5. Representative images of actin and myosin Va immunostaining in WT and DBA varicosities. *Top*: actin staining. Note that actin staining is seen in both WT and DBA varicosities. *Middle*: myosin Va staining. Note robust myosin Va staining in WT varicosities but absent staining in the DBA varicosities. *Bottom*: colocalization of myosin Va and actin. Note prominent colocalization of myosin Va with actin in WT varicosities. However, because of the lack of myosin Va, little colocalization of myosin Va and actin was seen in DBA varicosities. Slight adjustment in saturation of fluorescence was done for these representative images. Scale bars, 3 μm.

Quantitative comparison of fluorescence intensities after background correction was performed to compare SLC17A9 protein expression in WT and DBA varicosities. The fluorescence expression values in arbitrary units were normalized to the surface areas of the varicosities. WT and DBA enteric varicosities had similar expression of SLC17A9 (38.52 ± 3.53 in WT, 39.35 ± 3.04 in DBA, 2-tailed $P = 0.86$, unpaired *t*-test, $n = 70$ and 60 varicosities, respectively, from 6 independent pools of samples).

PLA of myosin Va with SLC17A9. In situ PLA was used to show signals for proteins localized at distances of <40 nm and indicating possible physical protein-protein interactions. In the WT mice varicosities, blobs of binding of myosin Va with SLC17A9 were clearly identified (Fig. 6*B*). Upon grayscale zooming, these stainings were seen both in perimembranous regions and across varicosities. These studies showed close proximity and possible binding of myosin Va with SLC17A9 reactive structures (possibly the ATP-containing vesicles). Omission of either primary antibody during the PLA assay resulted in absence of signal. In comparison, these binding signals were almost undetectable in enteric varicosities obtained from DBA mice because of the lack of myosin Va [9.83 ± 0.31 vs. 0.31 ± 0.07 (SE) blobs/varicosity, $n = 144$ and 159 WT and DBA varicosities, respectively, from 6 independent pools, $P < 0.0001$, 2-tailed unpaired *t*-test].

FM1–43 Labeling of Vesicles for Assay of Exoendocytosis Activity

To examine whether the defect in purinergic neurotransmission was likely due to defective exocytosis from varicosities, FM1–43 labeling of vesicles within the varicosities was performed. FM1–43 is a styryl dye that labels vesicles during their exocytosis when the inner membrane of the vesicle is exposed to the dye present in the extracellular space (17). With subsequent endocytosis, the stained vesicles accumulate inside the varicosity. Thus, the appearance of FM1–43-stained fluorescent speckles, after stimulation of the varicosities with KCl,

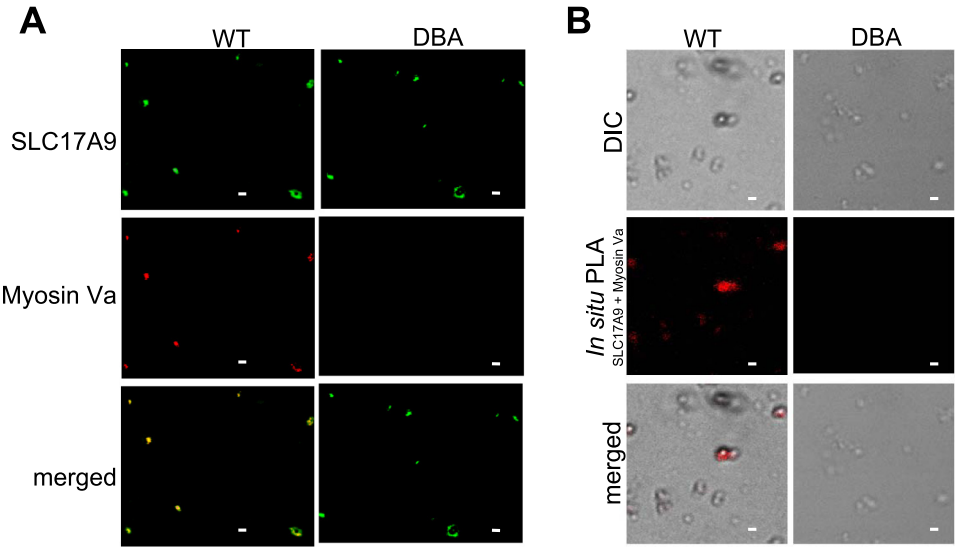

Fig. 6. Colocalization and in situ proximity ligation assay (PLA) of SLC17A9 with myosin Va in varicosities shows colocalization of SLC17A9 with myosin Va in WT but not in DBA mice. *Top*, *middle*, and *bottom* show immunostaining for SLC17A9, myosin Va, and merged images, respectively. Note that SLC17A9 signal expression in varicosities was similar in WT and DBA mice. Slight adjustment in saturation of fluorescence was performed for these representative images. *B*: in situ PLA of SLC17A9 with myosin Va. *Top*, DIC image. *Middle*, in situ PLA. *Bottom*, merged image. Red blobs indicate proximity of the two proteins at nm scales (<40 nm). Close proximity of myosin Va and SLC17A9 suggests that myosin Va may bind with the purinergic vesicles. Blobs were clearly seen in WT varicosities but only scantily in the DBA varicosities due to deficiency of myosin Va. Omission of SLC17A9 or myosin Va primary antibody did not result in a signal. Scale bars, 3 μm.

provides an estimate of active exoendocytosis cycle. In the WT varicosities, numerous clearly stained FM spots were observed in almost all varicosities in a field, each of which consists of several recycled synaptic vesicles. These observations indicate a high rate of exoendocytotic cycle. Compared with WT varicosities, varicosities from DBA mice showed scant FM1–43 staining, indicating scant exoendocytosis in myosin Va-deficient varicosities (Fig. 7). Quantitative comparison of FM1–43 fluorescence intensities after background correction was performed to quantitate efficiency of exocytosis. The fluorescence expression values in arbitrary units were normalized to surface areas of the varicosities. Compared with WT, DBA enteric varicosities had significantly lower FM1–43 staining intensities (48.06 ± 2.6 in WT vs. 5.03 ± 1.06 in DBA, 2-tailed $P < 0.0001$, unpaired *t*-test, $n = 2{,}924$ WT and 500 DBA varicosities obtained from 6 independent samples).

DISCUSSION

These studies show that: *1*) myosin Va-deficient DBA mice, compared with WT mice, show reduced pIJPs but normal hyperpolarizing responses to a selective P2Y1 receptor agonist. *2*) The vesicular ATP transporter SLC17A9 was localized to enteric varicosities in both WT and DBA. *3*) Varicosities obtained from DBA mice appeared normal but had reduced myosin Va. *4*) SLC17A9 was associated with myosin Va in WT varicosities but not in DBA varicosities. *5*) Vesicular exocytosis was reduced in myosin-deficient DBA varicosities.

In our preliminary studies, we observed that pIJPs were reduced in myosin-deficient DBA mice. Therefore, we systematically examined whether pIJP is suppressed in myosin-deficient DBA mice. Electric field stimulation under NANC conditions and masking of nitrergic responses revealed pIJP that was sensitive to a selective P2Y1 receptor antagonist, MRS-2279, suggesting that the pIJP was mediated by P2Y1 receptor. The purinergic neurotransmitter is thought to be ATP or a related purine. Recently, β-NAD rather than ATP has been suggested to be the purinergic transmitter. However, β-NAD was found to be a poor agonist of P2Y1 receptors 17(a). These observations do not support the view that β-NAD rather than ATP/ADP are purinergic neurotransmitters (18).

The pIJP was markedly suppressed in DBA mice compared with WT mice, indicating that myosin Va deficiency may impair purinergic neurotransmission. However, this impairment may result because of suppression of the neurotransmitter release or a postjunctional defect in clustering of P2Y1 receptors in smooth muscle cells. Myosin Va deficiency has been reported to impair targeting of receptors to membrane (36a).

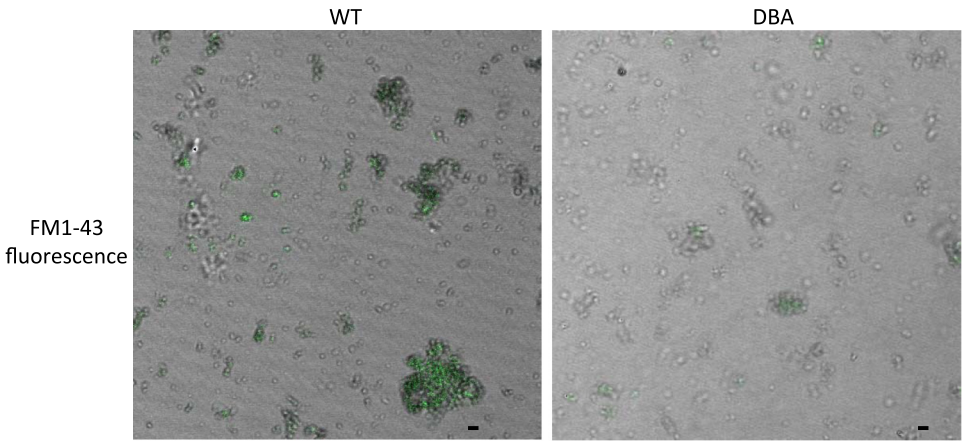

Fig. 7. Active exoendocytosis as determined by FM1–43 staining after stimulation of WT and DBA varicosities. Note that WT varicosities show robust staining with FM1–43 upon stimulation by 50 mM K^+. These varicosities were destained after prolonged stimulation with K^+ (images not shown). In contrast, DBA varicosities, stained simultaneously, showed little FM1–43 labeling, suggesting defective exoendocytosis. Images were acquired by intermittent laser scanning to prevent photobleaching. Scale bars, 3 μm.

The hyperpolarizing effect of the selective P2Y1 receptor agonist MRS-2365 on the smooth muscle cell was not reduced in the DBA mice, suggesting that the impaired pIJP was due to reduced prejunctional purinergic transmitter release rather than impaired smooth muscle responsiveness.

To understand the mechanism of impaired purinergic inhibitory neurotransmission in myosin deficiency, we performed studies on isolated enteric varicosities from WT and DBA mice to: *1*) identify purinergic varicosities; *2*) localize myosin Va in enteric varicosities and examine interaction of myosin Va with a purinergic vesicular marker; and *3*) investigate the effect of myosin deficiency on exocytosis of the vesicles.

The identity of purinergic varicosities has been investigated previously by a number of different techniques. The presence of purinergic nerve terminals is sometimes inferred by the release of purinergic transmitter from nerve muscle preparations (25, 51). However, investigation of the release of ATP in tissues is complicated by the fact that: *1*) ATP is released from almost all cell types; *2*) the released ATP is rapidly degraded by ectonucleotidases, which may complicate the interpretation of data on ATP release (25), and *3*) ATP is also released by a variety of nonexocytotic efflux pathways in many neural and nonneural cells (15, 25). Vesicular ATP has been identified by quinacrine fluorescence (1, 2), but this staining is not specific for adenine trinucleotides per se. Most recently, immunostaining for the SLC17A9 protein has been used to identify VNUT and hence the purinergic vesicles in a wide variety of mammalian neural and nonneural tissues (24, 29). SLC17A9 allows transmembrane transport and subsequent vesicular storage of ATP, ADP, and uridine nucleotides (40, 43). SLC17A9 is a highly specific transporter of ATP inside vesicular structures, and immunolocalization within nerve terminals strongly suggests existence of a vesicular release machinery for ATP (37, 39, 40, 46).

We used SLC17A9 to identify purinergic varicosities in preparation of enteric varicosities. We found that a vast majority of enteric varicosities immunostained for SLC17A9 and therefore were purinergic in nature. SLC17A9 does not transport β-NAD. Therefore, SLC17A9 immunostaining is consistent with ATP rather than β-NAD being the purinergic neurotransmitter at the prejunctional enteric nerve terminal (18). SLC17A9 staining showed that a very large proportion of the varicosities stained for ATP transporter.

The release of vesicular neurotransmitters requires membrane localization of the neurotransmitter-filled vesicles for exocytosis (36). The molecular motors for local transport of organelles are various myosins, including myosin Va. We have recently shown that myosin Va binds nNOSα to transport nNOSα to the varicosity membrane (12). The present study shows that myosin Va also plays a role in vesicular transport of purinergic varicosities. This is evidenced by the fact that: *1*) myosin Va is localized to enteric varicosities (12). This observation is supported by the fact that myosin Va has been shown to be present extensively in neurons, including the enteric neurons (14, 27). *2*) Myosin Va is associated with vesicles that stained for the SLC17A9, and PLA showed that myosin Va comes as close as 30–40 nm to SLC17A9, suggesting that ATP-containing vesicles are closely associated with myosin Va. This proximity may be due to myosin Va binding directly to SLC17A9 or a related supramolecular assembly involving vesicular membrane proteins like synaptobrevin, synaptophysin, and SV2 that are expressed on the surface of vesicles (34). These observations provide support for the hypothesis that myosin Va transports purinergic vesicles to the varicosity membrane for exocytosis and in myosin Va deficiency, membrane targeting and therefore vesicular exocytosis may be impaired.

We also compared vesicular exocytosis in WT and DBA mice using FM1–43 labeling. FM1–43 has been extensively used to study vesicular exocytosis (36). It is based on the principle that the extracellular styryl dye FM1–43 labels exocytotic vesicles whose inner membranes are exposed to the outside (17). During endocytosis of the labeled membranes, FM1–43-labeled vesicular endosomes are generated. Our studies show that, in myosin Va-deficient DBA mice, exoendocytosis of vesicles was reduced compared with WT varicosities. Taken together with other studies, these observations are consistent with the view that decreased targeting of purinergic vesicles to the varicosity membrane is responsible for decreased exocytosis in the face of normal content of the vesicles in varicosities in myosin-deficient DBA mice.

The inhibitory neurotransmission in the gut includes both P2Y1 receptor purinergic neurotransmission as well as nitrergic neurotransmission. Both of these types of transmissions have been reported to be impaired in myosin deficiency (12 and this study). Whereas purinergic transmission is dependent upon membrane targeting of purinergic vesicular exocytosis, nitrergic neurotransmission requires membrane targeting of the enzyme nNOSα. Purinergic vesicle as well as nNOSα may be cargos transported by myosin Va.

ATP and NO may be cotransmitters that are released from common "inhibitory" motor varicosities. Purinergic or nitrergic inhibitory neurotransmission was not completely lost in DBA mice. This may be due to the fact that DBA mice have only partial deficiency of myosin Va. It is also possible that compensation by some other myosin types may be involved in vesicular transport and exocytosis.

The present study shows that the impairment of vesicular exocytosis of enteric varicosities in myosin deficiency is associated with functional reduction in pIJP in gastric antrum. However, it is not known if other types of neuroeffector transmissions are also impaired in myosin Va deficiency. Further studies are needed to test this possibility. Further studies are also needed to determine if other myosin types serve as molecular motors for vesicles containing other neurotransmitters. It has been suggested that myosin II or myosin Vb rather than myosin Va serves as motors that target vesicles to membranes in glutamatergic synapses in cultured hippocampal neurons (26, 41) and presynaptic cholinergic nerve terminals in cultured superior cervical sympathetic ganglia (44).

SLC17A9 was localized to many varicosities, including those that were nNOSα negative. These observations are consistent with diffuse quinacrine staining in the enteric nerves (2) and widespread and extensive distribution of purinergic neurotransmission in the gut. The chemical nature of varicosities that are SLC17A9 positive but nNOSα negative is not fully understood. However, some of these varicosities may be varicosities of nNOS-positive descending interneurons. These nitrergic neurons exert their postsynaptic effects by releasing ATP and may utilize NO as a retrograde neurotransmitter (20). Further studies are required to test this possibility. SLC17A9 was also colocalized with vAChT. ATP and ACh serve as

cotransmitters at many sites (35). Further studies are needed to fully investigate the role of ATP as a cotransmitter with other neurotransmitters.

The findings of this study are of considerable clinical importance. Impairment of neurotransmission is a major underlying factor in a variety of motor disorders of various parts of the gut, the pathophysiology of most of which remains poorly understood. The search for causes of impaired neurotransmission is often focused on structural deficiency of nerves or the neurotransmitters (19). These studies show that impaired intracellular transport and proper intracellular localization of the secretory vesicles may also lead to functional deficiency of neurotransmission. Such deficiency occurs in the presence of normal-appearing neurotransmitter vesicles in the nerve terminals. The study of defects in intracellular motors, including myosin Va, may enhance our understanding and rational therapy of some of these motor disorders of the gut.

ACKNOWLEDGMENTS

We thank Antonietta D'Urso and Conor Stenerson for help during revision of the manuscript.

GRANTS

This work was supported by National Institute of Diabetes and Digestive and Kidney Diseases Grant DK-062867.

DISCLOSURES

Conflicts of interest: None.

REFERENCES

1. **Belai A, Burnstock G.** Evidence for coexistence of ATP and nitric oxide in non-adrenergic, non-cholinergic (NANC) inhibitory neurones in the rat ileum, colon and anococcygeus muscle. *Cell Tissue Res* 278: 197–200, 1994.
2. **Belai A, Burnstock G.** Pattern of distribution and co-localization of NOS and ATP in the myenteric plexus of human fetal stomach and intestine. *Neuroreport* 11: 5–8, 2000.
3. **Bennett MR.** Non-adrenergic non-cholinergic (NANC) transmission to smooth muscle: 35 years on. *Prog Neurobiol* 52: 159–195, 1997.
4. **Bridgman PC.** Myosin motor proteins in the cell biology of axons and other neuronal compartments. *Results Probl Cell Differ* 48: 91–105, 2009.
5. **Bridgman PC.** Myosin Va movements in normal and dilute-lethal axons provide support for a dual filament motor complex. *J Cell Biol* 146: 1045–1060, 1999.
6. **Brooks SA, Gabreski N, Miller D, Brisbin A, Brown HE, Streeter C, Mezey J, Cook D, Antczak DF.** Whole-genome SNP association in the horse: identification of a deletion in myosin Va responsible for Lavender Foal Syndrome. *PLoS Genet* 6: e1000909, 2010.
7. **Brown JR, Stafford P, Langford GM.** Short-range axonal/dendritic transport by myosin-V: a model for vesicle delivery to the synapse. *J Neurobiol* 58: 175–188, 2004.
8. **Burnstock G.** The journey to establish purinergic signalling in the gut. *Neurogastroenterol Motil* 20, *Suppl* 1: 8–19, 2008.
9. **Burnstock G.** Physiology and pathophysiology of purinergic neurotransmission. *Physiol Rev* 87: 659–797, 2007.
10. **Burnstock G.** Purinergic cotransmission. *Exp Physiol* 94: 20–24, 2009.
11. **Burnstock G, Campbell G, Satchell D, Smythe A.** Evidence that adenosine triphosphate or a related nucleotide is the transmitter substance released by non-adrenergic inhibitory nerves in the gut. *Br J Pharmacol* 40: 668–688, 1970.
12. **Chaudhury A, He XD, Goyal RK.** Myosin Va plays a key role in nitrergic neurotransmission by transporting nNOSα to enteric varicosity membrane. *Am J Physiol Gastrointest Liver Physiol* 301: G498–G507, 2011.
13. **Cheney RE, O'Shea MK, Heuser JE, Coelho MV, Wolenski JS, Espreafico EM, Forscher P, Larson RE, Mooseker MS.** Brain myosin-V is a two-headed unconventional myosin with motor activity. *Cell* 75: 13–23, 1993.
14. **Drengk AC, Kajiwara JK, Garcia SB, Carmo VS, Larson RE, Zucoloto S, Espreafico EM.** Immunolocalisation of myosin-V in the enteric nervous system of the rat. *J Auton Nerv Syst* 78: 109–112, 2000.
15. **Fields RD.** Nonsynaptic and nonvesicular ATP release from neurons and relevance to neuron-glia signaling. *Semin Cell Dev Biol* 22: 214–219, 2011.
16. **Foth BJ, Goedecke MC, Soldati D.** New insights into myosin evolution and classification. *Proc Natl Acad Sci USA* 103: 3681–3686, 2006.
17. **Gaffield MA, Betz WJ.** Imaging synaptic vesicle exocytosis and endocytosis with FM dyes. *Nat Protoc* 1: 2916–2921, 2006.

17a. **Gallego D, Gil V, Aleu J, Martinez-Cutillas M, Clavé P, Jimenez M.** Pharmacological characterization of purinergic inhibitory neuromuscular transmission in the human colon. *Neurogastroenterol Motil* 23: 792–e338, 2011.

18. **Goyal RK.** Evidence for beta-nicotinamide adenine dinucleotide as a purinergic, inhibitory neurotransmitter in doubt. *Gastroenterology* 141: e27, 2011.
19. **Goyal RK, Chaudhury A.** Pathogenesis of achalasia: lessons from mutant mice. *Gastroenterology* 139: 1086–1090, 2010.
20. **Gwynne RM, Bornstein JC.** Synaptic transmission at functionally identified synapses in the enteric nervous system: roles for both ionotropic and metabotropic receptors. *Curr Neuropharmacol* 5: 1–17, 2007.
21. **Hartman MA, Finan D, Sivaramakrishnan S, Spudich JA.** Principles of unconventional myosin function and targeting. *Annu Rev Cell Dev Biol* 27: 133–155, 2011.
22. **Huang JD, Brady ST, Richards BW, Stenolen D, Resau JH, Copeland NG, Jenkins NA.** Direct interaction of microtubule- and actin-based transport motors. *Nature* 397: 267–270, 1999.
23. **Jenkins NA, Copeland NG, Taylor BA, Lee BK.** Dilute (d) coat colour mutation of DBA/2J mice is associated with the site of integration of an ecotropic MuLV genome. *Nature* 293: 370–374, 1981.
24. **Larsson M, Sawada K, Morland C, Hiasa M, Ormel L, Moriyama Y, Gundersen V.** Functional and anatomical identification of a vesicular transporter mediating neuronal ATP release. *Cereb Cortex* In press.
25. **Lazarowski ER, Sesma JI, Seminario-Vidal L, Kreda SM.** Molecular mechanisms of purine and pyrimidine nucleotide release. *Adv Pharmacol* 61: 221–261, 2011.
26. **Lewis TL Jr, Mao T, Svoboda K, Arnold DB.** Myosin-dependent targeting of transmembrane proteins to neuronal dendrites. *Nat Neurosci* 12: 568–576, 2009.
27. **Marvin-Guy L, Lopes LV, Affolter M, Courtet-Compondu MC, Wagniere S, Bergonzelli GE, Fay LB, Kussmann M.** Proteomics of the rat gut: analysis of the myenteric plexus-longitudinal muscle preparation. *Proteomics* 5: 2561–2569, 2005.
28. **Mercer JA, Seperack PK, Strobel MC, Copeland NG, Jenkins NA.** Novel myosin heavy chain encoded by murine dilute coat colour locus. *Nature* 349: 709–713, 1991.
29. **Mihara H, Boudaka A, Sugiyama T, Moriyama Y, Tominaga M.** Transient receptor potential vanilloid 4 (TRPV4)-dependent calcium influx and ATP release in mouse oesophageal keratinocytes. *J Physiol* 589: 3471–3482, 2011.
30. **Miyata M, Kishimoto Y, Tanaka M, Hashimoto K, Hirashima N, Murata Y, Kano M, Takagishi Y.** A role for myosin Va in cerebellar plasticity and motor learning: a possible mechanism underlying neurological disorder in myosin Va disease. *J Neurosci* 31: 6067–6078, 2011.
31. **Mutafova-Yambolieva VN, Hwang SJ, Hao X, Chen H, Zhu MX, Wood JD, Ward SM, Sanders KM.** Beta-nicotinamide adenine dinucleotide is an inhibitory neurotransmitter in visceral smooth muscle. *Proc Natl Acad Sci USA* 104: 16359–16364, 2007.
32. **Osterweil E, Wells DG, Mooseker MS.** A role for myosin VI in postsynaptic structure and glutamate receptor endocytosis. *J Cell Biol* 168: 329–338, 2005.
33. **Panfoli I, Calzia D, Ravera S, Bianchini P, Diaspro A.** Immunochemical or fluorescent labeling of vesicular subcellular fractions for microscopy imaging. *Microsc Res Tech* 73: 1086–1090, 2010.
34. **Prekeris R, Terrian DM.** Brain myosin V is a synaptic vesicle-associated motor protein: evidence for a Ca2+-dependent interaction with the synaptobrevin-synaptophysin complex. *J Cell Biol* 137: 1589–1601, 1997.
35. **Qu ZD, Thacker M, Castelucci P, Bagyanszki M, Epstein ML, Furness JB.** Immunohistochemical analysis of neuron types in the mouse small intestine. *Cell Tissue Res* 334: 147–161, 2008.
36. **Rizzoli SO, Betz WJ.** Synaptic vesicle pools. *Nat Rev Neurosci* 6: 57–69, 2005.

36a. **Röder IV, Choi KR, Reischl M, Petersen Y, Diefenbacher ME, Zaccolo M, Pozzan T, Rudolf R.** Myosin Va cooperates with PKA RIα to mediate maintenance of the endplate in vivo. *Proc Natl Acad Sci USA* 107: 2031–3036, 2010.
37. **Rudnick G.** Vesicular ATP transport is a hard (V)NUT to crack. *Proc Natl Acad Sci USA* 105: 5949–5950, 2008.
38. **Rudolf R, Bittins CM, Gerdes HH.** The role of myosin V in exocytosis and synaptic plasticity. *J Neurochem* 116: 177–191, 2011.
39. **Sathe MN, Woo K, Kresge C, Bugde A, Luby-Phelps K, Lewis MA, Feranchak AP.** Regulation of purinergic signaling in biliary epithelial cells by exocytosis of SLC17A9-dependent ATP-enriched vesicles. *J Biol Chem* 286: 25363–25376, 2011.
40. **Sawada K, Echigo N, Juge N, Miyaji T, Otsuka M, Omote H, Yamamoto A, Moriyama Y.** Identification of a vesicular nucleotide transporter. *Proc Natl Acad Sci USA* 105: 5683–5686, 2008.
41. **Schnell E, Nicoll RA.** Hippocampal synaptic transmission and plasticity are preserved in myosin Va mutant mice. *J Neurophysiol* 85: 1498–1501, 2001.
42. **Seperack PK, Mercer JA, Strobel MC, Copeland NG, Jenkins NA.** Retroviral sequences located within an intron of the dilute gene alter dilute expression in a tissue-specific manner. *Embo J* 14: 2326–2332, 1995.
43. **Sreedharan S, Shaik JH, Olszewski PK, Levine AS, Schioth HB, Fredriksson R.** Glutamate, aspartate and nucleotide transporters in the SLC17 family form four main phylogenetic clusters: evolution and tissue expression. *BMC Genomics* 11: 17, 2010.
44. **Takagishi Y, Futaki S, Itoh K, Espreafico EM, Murakami N, Murata Y, Mochida S.** Localization of myosin II and V isoforms in cultured rat sympathetic neurones and their potential involvement in presynaptic function. *J Physiol* 569: 195–208, 2005.
45. **Thatte HS, He XD, Goyal RK.** Imaging of nitric oxide in nitrergic neuromuscular neurotransmission in the gut. *PLoS One* 4: e4990, 2009.
46. **Tokunaga A, Tsukimoto M, Harada H, Moriyama Y, Kojima S.** Involvement of SLC17A9-dependent vesicular exocytosis in the mechanism of ATP release during T cell activation. *J Biol Chem* 285: 17406–17416, 2010.
47. **Traba J, Satrustegui J, del Arco A.** Adenine nucleotide transporters in organelles: novel genes and functions. *Cell Mol Life Sci* 68: 1183–1206, 2011.
48. **Trybus KM.** Myosin V from head to tail. *Cell Mol Life Sci* 65: 1378–1389, 2008.
49. **Van Gele M, Dynoodt P, Lambert J.** Griscelli syndrome: a model system to study vesicular trafficking. *Pigment Cell Melanoma Res* 22: 268–282, 2009.
50. **Wagner W, Brenowitz SD, Hammer JA 3rd.** Myosin-Va transports the endoplasmic reticulum into the dendritic spines of Purkinje neurons. *Nat Cell Biol* 13: 40–48, 2000.
51. **White TD, Leslie RA.** Depolarization-induced release of adenosine 5′-triphosphate from isolated varicosities derived from the myenteric plexus of the guinea pig small intestine. *J Neurosci* 2: 206–215, 1982.